

# Spin and orbital magnetism in full Heusler alloys: A density functional theory study of $\text{Co}_2\text{YZ}$ ( $Y=\text{Mn, Fe}$ ; $Z=\text{Al, Si, Ga, Ge}$ )

Mahdi Sargolzaei, Manuel Richter, Klaus Koepernik, Ingo Opahle, and Helmut Eschrig  
*IFW Dresden, P.O. Box 270016, D-01171 Dresden, Germany*

Igor Chaplygin

*TU Dresden, Institut für Physikalische Chemie und Elektrochemie, D-01062 Dresden, Germany*

(Received 3 March 2006; revised manuscript received 31 August 2006; published 13 December 2006)

The effect of spin-orbit coupling and orbital polarization (OP) corrections on the spin and orbital magnetism of full Heusler alloys is investigated by means of local spin-density calculations. It is demonstrated that OP corrections are needed to explain the experimental orbital moments  $M_l$ . Model calculations employing one ligand field parameter yield the correct order of magnitude of  $M_l$ , but do not account for its quantitative composition dependence. Spin-orbit coupling reduces the degree of spin polarization of the density of states at Fermi level by a few percent. We provide arguments that  $\text{Co}_2\text{MnGa}$  and the  $\text{Co}_2\text{YZ}$  compounds with  $Y=\text{Fe}$  might not be half metals as suggested by recent experiments for  $Z=\text{Si}$ .

DOI: [10.1103/PhysRevB.74.224410](https://doi.org/10.1103/PhysRevB.74.224410)

PACS number(s): 75.30.-m, 71.20.Lp

## I. INTRODUCTION

Intense experimental<sup>1–4</sup> and theoretical<sup>5–8</sup> efforts have been devoted to Heusler alloys<sup>9</sup> recently. An intriguing property, disclosed for  $\text{Co}_2\text{YZ}$  Heusler compounds by Kübler *et al.*,<sup>10</sup> is so-called half metallic ferromagnetism,<sup>11</sup> where one spin band is metallic and the other is semiconducting. Much of the recent interest is just due to this feature,<sup>12</sup> a 100% spin polarization at Fermi level that promises potential application in spin-electronic devices. It is, however, frequently overlooked that half metallicity is bound to well-ordered bulk compounds in most cases<sup>13</sup> and considerable experimental difficulties often prevent the preparation of well-ordered thin films<sup>14</sup> as a precondition for the desired application.

Apart from the mentioned application-driven interest, the magnetism of ideally ordered bulk Heusler compounds still poses a challenge to the theoretical understanding of electronic structure. If orbital magnetism is neglected, any half metallic ground state is invariant with zero Pauli susceptibility in an external field smaller than a critical field.<sup>15</sup> It is also obvious that the spin magnetic moment per unit cell in such a state must be integer. A number of other, system-specific theoretical<sup>10,16–19</sup> and experimental studies<sup>20,21</sup> of spin-only magnetism leading to half metallicity of the full Heusler alloys have been published. On the other hand, less attention has been paid in the past to the orbital degrees of freedom in these compounds. It is clear that the concept of half metallicity neglects spin-orbit coupling. For instance, neither complete spin polarization at the Fermi level nor integer magnetic moments can be expected if spin-orbit coupling is taken into account.<sup>22,23</sup> It is thus interesting to study the magnitude of the related deviations from the idealized case.

Commonly, ligand fields largely quench the orbital magnetic moment in cubic systems containing  $3d$  transition metals. Elmers *et al.*<sup>24</sup> have shown in their x-ray magnetic circular dichroism (XMCD) studies, however, that the orbital moment in the cubic  $\text{Co}_2\text{FeAl}$  full Heusler compound is quite sizeable,  $M_l \approx 0.5 \mu_B/\text{f.u.}$ , and even somewhat larger

values were reported for this compound in a more recent study by the same group.<sup>26</sup> With the same method, Miyamoto *et al.* and Wurmehl *et al.* also found noticeable orbital moments in  $\text{Co}_2\text{MnGe}$  (Ref. 27) and in  $\text{Co}_2\text{FeSi}$ ,<sup>28</sup> respectively.

Galanakis<sup>30</sup> considered the orbital magnetic moments of different Heusler compounds in a theoretical approach using the local (spin) density approximation [L(S)DA]. He employed a fully relativistic Korringa-Kohn-Rostoker (KKR) multiple-scattering Green's function method and found very small orbital magnetic moments on each constituent. Compared with the mentioned experimental results, the orbital moments found by Galanakis are smaller by factors of 2–4. This problem was also observed for the alloy system  $\text{Co}_2\text{Cr}_{1-x}\text{Fe}_x\text{Al}$  by Wurmehl *et al.*, who found<sup>26</sup> only a slight improvement by using OP corrections, and for  $\text{Co}_2\text{FeSi}$  by the same group. In the latter case, neither OP corrections nor relativistic LDA+ $U$  calculations could close the gap between measured and calculated orbital moments, though both approximations improved the mismatch in comparison with LSDA.<sup>28</sup>

With the intention to resolve this discrepancy, we focus the present investigation on  $\text{Co}_2\text{YZ}$  full Heusler compounds with  $Y=\text{Mn}$  or  $\text{Fe}$ ;  $Z=\text{Al, Ga, Si, or Ge}$ . All combinations of these elements are considered. Some of them, such as  $\text{Co}_2\text{MnSi}$  and  $\text{Co}_2\text{MnGe}$ , were found to be half metallic in earlier electronic structure calculations.<sup>17</sup> We study the magnetic and electronic properties of these eight compounds with a particular emphasis on the influence of spin-orbit coupling and orbital magnetism. The underestimation of orbital moments in the LSDA approach reported by Galanakis and Wurmehl is confirmed. We demonstrate, however, that explicit consideration of orbital polarization effects brings theoretical and experimental data systematically in better coincidence. Finally, we suggest an alternative explanation for the recently<sup>28</sup> measured magnetic moment of  $\text{Co}_2\text{FeSi}$  that can resolve the apparent discrepancy between the two experimental facts of integer total moment and large orbital moment.

The paper is organized as follows: Section II contains details about the crystal structure and the numerics. Section III presents the results and discussion (calculated spin moments, orbital moments, a qualitative model for the orbital moments, volume dependent properties of Co<sub>2</sub>FeSi, and remarks about half metallicity). Finally, the paper is summarized in Sec. IV.

## II. CRYSTAL STRUCTURE AND COMPUTATIONAL DETAILS

The considered full Heusler alloys Co<sub>2</sub>YZ adopt the ordered L2<sub>1</sub>-type structure (space group  $Fm\bar{3}m$ ), which may be understood as the result of four interpenetrating face-centered-cubic (fcc) lattices. The Y and Z atoms occupy two fcc sublattices with origin at (0 0 0) and (1/2 1/2 1/2), respectively. The Co atoms are located in sublattices with origins at (1/4 1/4 1/4) and (3/4 3/4 3/4).

We have carried out density functional calculations<sup>31</sup> using the relativistic version<sup>32</sup> of the full-potential local-orbital (FPLO) minimum-basis band-structure method.<sup>33</sup> In this scheme the four-component Kohn-Sham-Dirac (KSD) equation, which implicitly contains spin-orbit coupling up to all orders, is solved self-consistently. For the present calculations, the following states were included in the valence basis: the  $3s3p;3d4s4p$  states of Co, Mn, Fe, Ga, and Ge and the  $2s2p;3s3p;3d$  states of Al and Si. The inclusion of Ga, Ge, and transition metals  $3s$  and  $3p$  semicore states together with  $2s$  and  $2p$  semicore states of Al and Si into the valence basis was used to account for their non-negligible overlap with neighboring core states. The Al and Si  $3d$  polarization states were used to improve the completeness of the basis set. All radial basis states are provided numerically on a grid and adjusted to the potential in each iteration step. The site-centered potentials and densities were expanded in spherical harmonic contributions up to  $l_{max}=12$ . The convergence of the total energies ( $10^{-6}$  hartree) with respect to the  $k$ -space integrations was checked separately for each of the considered Heusler alloys. We found that  $30 \times 30 \times 30 = 27\,000$   $k$  points in the full Brillouin zone were sufficient in all cases. The related stability of charge and magnetic population numbers was better than  $10^{-4}$ .

The Perdew-Wang parametrization<sup>34</sup> of the exchange-correlation (XC) potential in the LSDA was used. In the local spin-density approximation for bcc Fe and hcp Co, magnetic spin moments are obtained within typically 5% deviation from experiment. On the other hand, the orbital moments of Fe and Co are found a factor of 2 smaller compared with experimental values in this approach. For a better description of orbital magnetism in the  $d$  shell of Fe and Co atoms, different orbital polarization OP corrections to LSDA have been suggested (see Ref. 35 for an overview). Here, an OP correction term for an unfilled  $l$  shell as far as possible derived from KSD theory by Eschrig *et al.*<sup>36</sup> is added to the LSDA exchange and correlation energy functional:

$$E_l^{\text{OP(b)}} = -\frac{1}{2} \sum_{\sigma} p_l N_{\sigma} \left( l + \frac{1 - N_{\sigma}}{2} \right) M_{l\sigma}^2, \quad (1)$$

$$M_{l\sigma} = \sum_{k,m} n_k \langle \psi_k | \varphi_{m\sigma} \rangle m \langle \varphi_{m\sigma} | \psi_k \rangle, \quad (2)$$

$$N_{\sigma} = \sum_k n_k |\langle \psi_k | \varphi_{m\sigma} \rangle|^2, \quad (3)$$

where  $\sigma = \uparrow (\downarrow)$  denotes the majority (minority) spin direction. The variables  $n_k$ ,  $\psi_k$ , and  $\varphi_{m\sigma}$  are occupation numbers, KSD bispinor orbitals, and scalar local  $l$  basis functions, respectively. The  $l$  and  $m$  denote azimuthal and magnetic quantum numbers, and the  $M_{l\sigma}$  are angular momentum expectation values. The coefficient  $p_l$  slightly linearly increases within a shell. For Mn, Fe, and Co, the related numbers are 56.0, 57.6, 59.2 meV, respectively. In order to compare our results with a frequently employed empirical OP correction suggested by Eriksson *et al.*,<sup>37</sup> in a spin-dependent form for incompletely filled  $d$  shells, we alternatively added a term  $E_l^{\text{OP(a)}} = -\sum_{\sigma} B_{l\sigma} M_{l\sigma}^2 / 2$  to the total energy functional. Here,  $B_{l\sigma}$  is the related Racah parameter.<sup>35</sup> The final values of spin and orbital moments are obtained from corresponding projections on the atomic basis states.<sup>32</sup>

## III. RESULTS AND DISCUSSION

We optimized the equilibrium lattice parameters using LSDA total-energy calculations. The calculated lattice constants  $a$  are 2–3 % smaller than the experimental (mostly, room-temperature) values,<sup>38</sup> see Table I. Such deviations are common in the LSDA. We also checked that the OP corrections do not significantly change the evaluated lattice constants. If not indicated otherwise, the LSDA lattice constants are used in the further calculations in order to be model consistent. The LSDA and LSDA+OP spin and orbital moments for each single constituent are summarized in Table I.

### A. Calculated spin moments

OP corrections turned out to influence the spin moments only marginally. Thus we discuss only LSDA spin moments (Table I). As expected, the Mn and Fe atoms as Y components carry the largest spin moments ( $2.65\mu_B - 3.09\mu_B$ ) in the considered compounds. The  $sp$  atoms are weakly spin polarized and couple antiferromagnetically with Mn, Fe, and Co. One should note that the Mn and Co spin moments in the case of Co<sub>2</sub>MnZ increase when we substitute Si for Al or Ge for Ga. This is in accordance with the Slater-Pauling behavior<sup>39</sup> discussed by Galanakis *et al.*<sup>19</sup> The total spin magnetic moments of Co<sub>2</sub>MnAl, Co<sub>2</sub>MnSi, and Co<sub>2</sub>MnGe are very close to an integer value ( $4\mu_B$ ,  $5\mu_B$ , and  $5\mu_B$ , respectively). In particular, Co<sub>2</sub>MnSi and Co<sub>2</sub>MnGe are found to be half metals in the calculations, if spin-orbit coupling is neglected. The tiny deviation from integer Bohr magneton number is due to spin-orbit coupling that slightly reduces the spin moment. The compound Co<sub>2</sub>MnAl is very close to half metallicity (see Fig. 1, and Table IV) without spin-orbit coupling, while the isoelectronic Co<sub>2</sub>MnGa is not a half metal in our approach. The probable reason for this dissimilarity is the larger size of the Ga atom compared with the Al atom that leads to a stronger hybridization with the transition-

TABLE I. Spin ( $M_s$ ) and orbital ( $M_l$ ) moments for constituents of the  $\text{Co}_2\text{YZ}$  full Heusler alloys together with total spin and total orbital moments and their sum, calculated at the LSDA lattice constant. The first line for each compound gives the LSDA results and related model results (see text) in parentheses. Lines with the indices a and b show results of calculations with orbital polarization corrections suggested by Eriksson *et al.* (Ref. 37) and by Eschrig *et al.* (Ref. 36) added to the LSDA-XC energy functional, respectively. The last two columns are the theoretical and experimental lattice constants in atomic units (a.u.). The influence of OP corrections on the spin moments and on the lattice constants is marginal and left out of the table. The experimental lattice constants are taken from Villars *et al.* (Ref. 38).

$\text{Co}_2\text{YZ}$	$M_s^{\text{Co}}$	$M_l^{\text{Co}}$	$M_s^{\text{Y}}$	$M_l^{\text{Y}}$	$M_s^{\text{Z}}$	$M_s^{\text{total}}$	$M_l^{\text{total}}$	$M^{\text{total}}$	$a^{\text{LSDA}}$	$a^{\text{expt.}}$
$\text{Co}_2\text{MnAl}$	0.740	0.014 (0.068)	2.650	0.010	-0.133	3.997	0.038	4.035	10.56	10.88
a		0.023		0.008			0.054	4.051		
b		0.027		0.007			0.061	4.058		
$\text{Co}_2\text{MnSi}$	1.022	0.029 (0.077)	3.028	0.010	-0.078	4.994	0.069	5.063	10.44	10.69
a		0.040		0.013			0.095	5.089		
b		0.045		0.015			0.107	5.101		
$\text{Co}_2\text{MnGa}$	0.715	0.011 (0.067)	2.698	0.014	-0.089	4.039	0.036	4.075	10.56	10.91
a		0.020		0.013			0.053	4.092		
b		0.024		0.017			0.065	4.104		
$\text{Co}_2\text{MnGe}$	0.978	0.031 (0.065)	3.089	0.015	-0.050	4.995	0.078	5.073	10.62	10.86
a		0.044		0.020			0.109	5.104		
b		0.049		0.023			0.122	5.117		
$\text{Co}_2\text{FeAl}$	1.116	0.050 (0.058)	2.704	0.040 (0.051)	-0.098	4.838	0.140	4.978	10.54	10.83
a		0.058		0.072			0.189	5.027		
b		0.067		0.082			0.217	5.055		
$\text{Co}_2\text{FeSi}$	1.198	0.038 (0.065)	2.671	0.072 (0.031)	-0.034	5.033	0.149	5.182	10.40	10.67
a		0.053		0.127			0.235	5.268		
b		0.060		0.159			0.281	5.314		
$\text{Co}_2\text{FeGa}$	1.114	0.040 (0.056)	2.738	0.054 (0.061)	-0.061	4.905	0.134	5.039	10.56	10.84
a		0.060		0.077			0.197	5.102		
b		0.071		0.090			0.232	5.137		
$\text{Co}_2\text{FeGe}$	1.257	0.045 (0.067)	2.752	0.080 (0.038)	0.006	5.272	0.170	5.442	10.60	10.85
a		0.063		0.140			0.267	5.539		
b		0.074		0.184			0.333	5.605		

metal valence states and a related broadening of the bands, see Fig. 1. The gap in the minority spin density of states is more narrow than the related gap of  $\text{Co}_2\text{MnAl}$  and the broadened minority states cross the Fermi level. A different situation is found for the case of  $\text{Co}_2\text{MnSi}$  and  $\text{Co}_2\text{MnGe}$ . Here, the Fermi level is situated close to the unoccupied minority states since the number of valence electrons is by 1 larger than in the  $\text{Co}_2\text{MnAl}$  and  $\text{Co}_2\text{MnGa}$  compounds. Thus the gap narrowing by replacing Si with Ge does not destroy the half metallicity.

The  $\text{Co}_2\text{FeZ}$  compounds are normal ferromagnetic metals with both majority and minority bands crossing the Fermi level, see Fig. 1. The Fe and Co spin moments are less affected by changing the alloying element Z in these compounds and the total spin moment stays close to  $5\mu_B$  per formula unit. This behavior violates the Slater-Pauling behavior, as it was already discussed by Galanakis *et al.* for the two cases of  $\text{Co}_2\text{FeAl}$  and  $\text{Co}_2\text{FeSi}$ .<sup>19</sup> The particular case of  $\text{Co}_2\text{FeSi}$  is discussed in more detail in Sec. III D.

### B. Orbital moments

Total and site-resolved orbital moments calculated in different approximations are given in Table I. Relativistic

LSDA produces orbital moments induced from spin polarization via spin-orbit coupling. Our LSDA calculated orbital moments are in a very good agreement (within a deviation of  $0.005\mu_B$  or less) with the orbital moments evaluated for four of the considered compounds by Galanakis.<sup>30</sup>

The orbital moments are in all cases small compared with the spin moments as it is usual in cubic  $3d$  transition metals. In particular, the Mn orbital moments are tiny since the Mn  $3d$  shell is close to half filling. Comparing the orbital moments of Fe and Co in  $\text{Co}_2\text{FeZ}$  with those of Mn and Co in  $\text{Co}_2\text{MnZ}$  reveals that the former are considerably larger.

To our knowledge, there are only three XMCD experiments to determine orbital moments for the considered compounds. Since the ratio  $M_l/M_s$  is more closely related to the original experimental data than the individual moments, we compare experimental and theoretical results of this ratio in Table II. It should be pointed out that the analysis of the XMCD experiments give forth the ratio  $M_l/(M_s - 7\langle T_z \rangle)$ . The magnetic dipole term  $\langle T_z \rangle$  comes about by the anisotropy of the atomic spin density due to spin-orbit coupling or ligand field effects.<sup>40-42</sup> However, for  $3d$  transition-metal atoms in a cubic environment, the  $7\langle T_z \rangle$  is typically by a factor of about  $10^{-3}$  smaller than the spin magnetic moment  $M_s$ ,<sup>26,43</sup> and

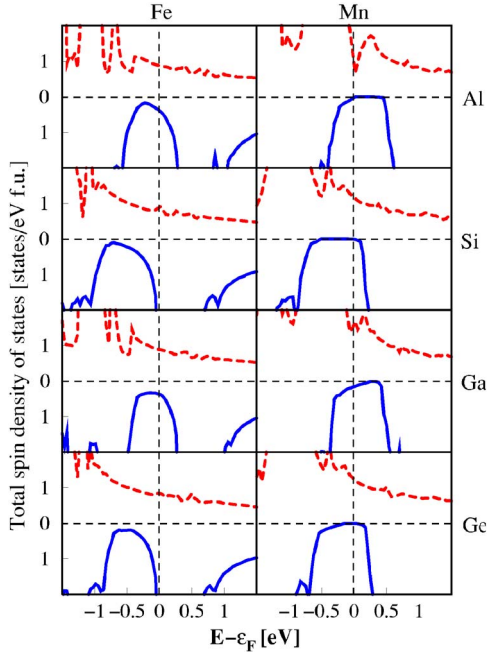


FIG. 1. (Color online) Total densities of states of all considered compounds close to the Fermi level, obtained by fully relativistic LSDA calculations. Majority (minority) spin channels with dashed red (solid blue) lines are shown in the upper (lower) parts of the individual panels.

therefore can be neglected in the considered cubic compounds.

From their XMCD studies, Miyamoto *et al.* obtained a ratio of about 0.07 for Co and of about 0.01 for Mn in  $\text{Co}_2\text{MnGe}$ .<sup>27</sup> The Co value is more than two times larger than that obtained by our LSDA calculation, 0.03. The same LSDA value has been found by Galanakis *et al.*,<sup>30</sup> and an even smaller value of about 0.02 has been obtained by Picozzi *et al.*,<sup>17</sup> by means of generalized gradient approximation FLAPW calculations. However, when we compare the orbital magnetic moments calculated with the two variants of OP corrections ( $0.044\mu_B/\text{Co}$  and  $0.049\mu_B/\text{Co}$ , Table I) which account for the direct nonrelativistic interaction of the

orbital moments with the inner field, they are in a much better agreement with experiment. This enhancement to about 0.05 is slightly dependent on the lattice constant, Table II. Also, the LSDA+OP ratios for Mn are almost equal to the experimental value of 0.01, whereas the related LSDA results are smaller (0.005 in our calculation, 0.007 in Ref. 30, and 0.003 in Ref. 17).

A further XMCD study was recently carried out on quaternary alloys by Elmers *et al.*, including the case of  $\text{Co}_2\text{FeAl}$ .<sup>24,25</sup> They found that the ratios of  $M_l/M_s$  for Co and Fe are  $0.14 \pm 0.02$  and  $0.06 \pm 0.02$ , respectively. These ratios are found to be 0.045 for Co and 0.015 for Fe in our LSDA calculations. Even the application of OP corrections results in values that are roughly two times smaller than the experimental values.

Most recently, an XMCD experiment was reported by Wurmehl *et al.* for  $\text{Co}_2\text{FeSi}$ .<sup>28</sup> Their  $M_l/M_s$  ratios, extrapolated to 0 K, are 0.1 for Co and 0.05 for Fe, respectively. Our corresponding LSDA ratios amount to 0.032 for Co and 0.027 for Fe. Using the two variants of OP corrections reveals a very good agreement with the experimental value for Fe, but both of them give two times smaller values than the experiment for Co (about 0.05–0.06 for both elements). It should be noted that our result is closer to the experimental result for Fe than the LDA+ $U$  result given in Ref. 28 (0.05 for Co and 0.02 for Fe, respectively).

Summarizing this section, orbital polarization corrections reduce the difference between calculated and measured ratios  $M_l/M_s$  in comparison to plain LSDA for all six considered cases. In the mean, LSDA yields about 40% of the measured ratio, while LSDA+OP(b) yields about 70%, with moderate sensitivity to the choice of the lattice parameter.

### C. Ligand field model for the orbital moments

In order to better understand the origin of the relatively small but yet different orbital moments of Co, Mn, and Fe in the distinct Heusler alloys compiled in Table I, we performed a simple model calculation for the LSDA orbital moment of the  $3d$  shell, based on the model described in Ref. 44. The value of the orbital moment is determined by an interplay

TABLE II. Comparison of available experimental (XMCD) and calculated ratios  $M_l/M_s$ . Calculated data obtained by LSDA and LSDA+OP(b) (Ref. 36) are given for both LSDA and experimental lattice constants.

Element in compound	Expt.	LSDA at $a^{\text{LSDA}}$	LSDA+OP(b) at $a^{\text{LSDA}}$	LSDA at $a^{\text{expt.}}$	LSDA+OP(b) at $a^{\text{expt.}}$
Co in $\text{Co}_2\text{MnGe}$	0.07 <sup>a</sup>	0.032	0.050	0.034	0.056
Mn in $\text{Co}_2\text{MnGe}$	0.01 <sup>b</sup>	0.005	0.007	0.006	0.008
Co in $\text{Co}_2\text{FeAl}$	$0.14 \pm 0.02^c$	0.045	0.060	0.041	0.072
Fe in $\text{Co}_2\text{FeAl}$	$0.06 \pm 0.02^d$	0.015	0.030	0.020	0.033
Co in $\text{Co}_2\text{FeSi}$	0.1 <sup>e</sup>	0.032	0.050	0.037	0.064
Fe in $\text{Co}_2\text{FeSi}$	0.05 <sup>f</sup>	0.027	0.060	0.026	0.050

<sup>a</sup>Reference 27.

<sup>b</sup>Reference 27.

<sup>c</sup>Reference 24 and 25.

<sup>d</sup>Reference 24 and 25.

<sup>e</sup>Reference 28.

<sup>f</sup>Reference 28.

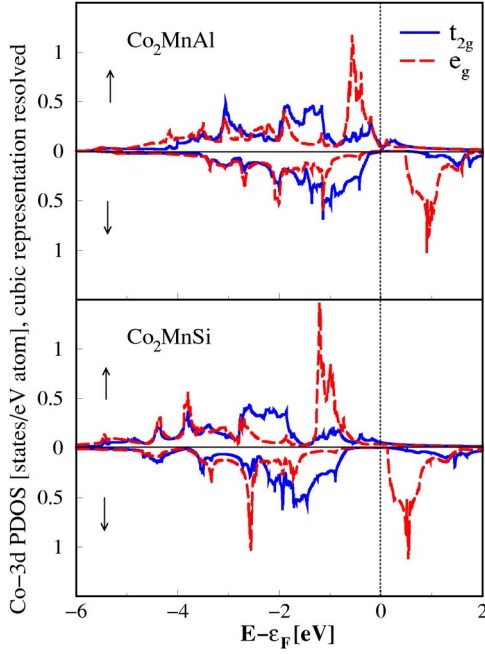


FIG. 2. (Color online) Co 3d partial DOS for  $\text{Co}_2\text{MnAl}$  (upper panel) and  $\text{Co}_2\text{MnSi}$  (lower panel). The threefold degenerate  $t_{2g}$  (twofold degenerate  $e_g$ ) states are shown with dashed red (solid blue) lines in majority ( $\uparrow$ ) and minority ( $\downarrow$ ) spin subshell.

between the ligand field and the spin-orbit coupling. The ligand field splitting tends to quench the orbital moment while spin-orbit interaction partially restores it. Since the systems at hand are cubic, the ligand field splits the five-fold degenerate 3d spin subshell in threefold degenerate  $t_{2g}$  states ( $|yz\rangle, |zx\rangle, |xy\rangle$ ) and twofold degenerate  $e_g$  states ( $|x^2 - y^2\rangle, |3z^2 - r^2\rangle$ ) in the standard notation of real  $d$  orbitals. Each of the real spherical harmonics has zero orbital moment. Figure 2 shows this situation for two examples,  $\text{Co}_2\text{MnAl}$  and  $\text{Co}_2\text{MnSi}$ , in the absence of spin-orbit coupling. Assuming the quantization axes for spin and orbital moments to be the same ( $z$  direction) and the majority spin projection to be positive, the Hamiltonian matrix of the sum of spin-orbit and ligand field interactions in the subspace of the  $t_{2g}$  and  $e_g$  functions for minority spin reads

$$\begin{pmatrix} |yz\rangle: & 0 & -i\xi/2 & 0 & 0 & 0 \\ |zx\rangle: & +i\xi/2 & 0 & 0 & 0 & 0 \\ |xy\rangle: & 0 & 0 & 0 & -i\xi & 0 \\ |x^2 - y^2\rangle: & 0 & 0 & i\xi & \Delta & 0 \\ |3z^2 - r^2\rangle: & 0 & 0 & 0 & 0 & \Delta \end{pmatrix}, \quad (4)$$

where  $\Delta$  is the ligand field splitting between the  $e_g$  and  $t_{2g}$  levels and  $\xi \sum_i \hat{l}_{z,i} \hat{s}_{z,i}$  is the spin-orbit coupling operator with the positive spin-orbit coupling constant  $\xi$ . Under the condition  $\xi \ll \Delta$ , which is usually fulfilled in 3d transition metals, the new minority  $t_{2g}$ -like eigenstates have energies  $-\xi/2$ ,  $-\xi^2/\Delta$ , and  $\xi/2$  and the  $e_g$ -like eigenstates have energies  $\Delta$  and  $\Delta + \xi^2/\Delta$ . The orbital moment is calculated by the following approximate expression:

$$M_l = - \sum_{\sigma=\uparrow,\downarrow} \sum_{i=1}^5 \langle l_z \rangle_i \times \text{sgn}(\sigma) \int_{-\infty}^{\epsilon_F} \text{PDOS}(i, \sigma) dE, \quad (5)$$

where  $\langle l_z \rangle_i = 1, 4\xi/\Delta, -1$  are the orbital moment projections of the minority  $t_{2g}$ -like new eigenstates and  $\langle l_z \rangle_i = 0, -4\xi/\Delta$  are the orbital moment projections of the minority  $e_g$ -like new eigenstates. PDOS is the partial density of states for the  $t_{2g}$ -like and  $e_g$ -like new eigenstates.

Using a calculated spin-orbit coupling constant  $\xi$  of 0.054 (0.045) eV for Co (Fe) and typical ligand field splitting  $\Delta$  of 1 eV, we obtained the numbers given in parentheses in Table I. These orbital magnetic moments are in qualitative agreement with the orbital moments obtained by the full calculation, though the individual numbers differ by factors up to 6. While the model provides the principal mechanisms of spin-orbit coupling on the orbital moment, the reason for the deviations lies in the simplification of the model Hamiltonian, where the action of the ligand field is described by a single parameter. The densities of states presented in Fig. 2 show that this approximation is not well justified:  $t_{2g}$  and  $e_g$  states are not simply split but exhibit considerably different shapes of the DOS.

Another, yet more simplified, model was suggested some time ago by Eriksson *et al.*<sup>45</sup> and, in parallel, by Ebert *et al.*<sup>46</sup> In that model, spin-orbit coupling was assumed to shift the  $m_l$  subbands rigidly. Such a shift yields negative orbital moment contributions in the majority spin subband and positive orbital moment contributions in the minority spin subband, in accordance with the third Hund's rule. Applied to half metals, a rigid shift would give zero orbital moment contribution for the spin channel which has a gap at the Fermi level. That means the rigid shift model would provide negative orbital moments for at least the two half metallic compounds considered here, in contradiction with the full calculations and with experiment on  $\text{Co}_2\text{MnGe}$ .

As a consequence, the change of the orbital moment projection of the states due to spin-orbit coupling considered in the present model, Eq. (4), is crucial for obtaining the correct sign of the orbital moment. The values given in Table I are composed of relatively large (about  $0.3\mu_B$ ) and almost compensating contributions from the two spin channels. Thus the quantitative result is sensitive to the discussed simplification of the model.

#### D. Volume dependent properties of $\text{Co}_2\text{FeSi}$

The compound  $\text{Co}_2\text{FeSi}$  went into the focus of interest recently, when Wurmehl *et al.* measured a large total magnetic moment of about  $6\mu_B$ .<sup>28</sup> This value, which is higher than previously measured values of  $5.18\mu_B$  (Ref. 47) and  $5.7\mu_B$  (Ref. 48) indicates half metallic behavior. Indeed, related LDA+ $U$  calculations yield a gap in the minority spin DOS at the Fermi level and a total moment of  $6\mu_B$ . It was concluded that  $\text{Co}_2\text{FeSi}$  is a half metal with important correlation effects.<sup>28,29</sup> On the other hand, both LSDA and LSDA+OP calculations yield much smaller total moments, ( $\sim 5.2\mu_B - 5.3\mu_B$ ) at theoretical lattice constant, see Table I, and a large DOS in both spin channels, see Fig. 1.

TABLE III. Comparison of available experimental and calculated total magnetic moments per formula unit. Calculated data obtained by LSDA and LSDA+OP(b) are given for both LSDA and experimental lattice constants. The degree of order within the  $L2_1$  structure has not always been analyzed. All experimental data were obtained at low temperature.

Compound	$M_{\text{exp}}^{\text{tot}}$	$M_{\text{LSDA}}^{\text{tot}}$ at $a^{\text{LSDA}}$	$M_{\text{OP(b)}}^{\text{tot}}$ at $a^{\text{LSDA}}$	$M_{\text{LSDA}}^{\text{tot}}$ at $a^{\text{exp}}$	$M_{\text{OP(b)}}^{\text{tot}}$ at $a^{\text{exp}}$
Co <sub>2</sub> MnAl	4.01 ± 0.05 <sup>a</sup>	4.035	4.058	4.066	4.095
Co <sub>2</sub> MnSi	4.90, <sup>b</sup> 5.07 ± 0.05 <sup>c</sup>	5.063	5.101	5.071	5.114
Co <sub>2</sub> MnGa	4.05 ± 0.05 <sup>d</sup>	4.075	4.104	4.150	4.162
Co <sub>2</sub> MnGe	4.93, <sup>e</sup> 5.11 ± 0.05 <sup>f</sup>	5.073	5.117	5.078	5.129
Co <sub>2</sub> FeAl	4.96, <sup>g</sup> 5.29 <sup>h</sup>	4.978	5.055	5.083	5.193
Co <sub>2</sub> FeSi	5.18, <sup>i</sup> 5.7, <sup>j</sup> 5.97 ± 0.05 <sup>k</sup>	5.182	5.314	5.664	5.800
Co <sub>2</sub> FeGa	5.13, <sup>l</sup> 5.15 <sup>m</sup>	5.039	5.137	5.149	5.270
Co <sub>2</sub> FeGe	5.54 <sup>n</sup>	5.442	5.605	5.700	5.857

<sup>a</sup>80% B2 structure, Ref. 49.

<sup>b</sup>Reference 47.

<sup>c</sup>Reference 49.

<sup>d</sup>Reference 49.

<sup>e</sup>Reference 47.

<sup>f</sup>Reference 49 and 50.

<sup>g</sup>Reference 47.

<sup>h</sup>Reference 25.

<sup>i</sup>Reference 47.

<sup>j</sup>Disordered DO<sub>3</sub> structure, Ref. 48.

<sup>k</sup>Reference 28.

<sup>l</sup>Reference 47.

<sup>m</sup>Reference 21.

<sup>n</sup>Reference 47.

The question arises of why this compound shows strong correlation effects, while the other, chemically very similar, compounds are well described by LSDA(+OP) theory. This fact is demonstrated in Table III, where experimental total moments are compared with total moments calculated at both theoretical and experimental lattice constants. Concerning the Mn-containing compounds it can be stated that the agreement between experiment and theory is within two times the experimental error bounds (including the scatter of experimental results) for both choices of lattice parameters and for both LSDA and LSDA+OP approaches.

The situation is less satisfactory for the Fe-containing compounds. Here, on the one hand, significant scatter in the experimental data is found, pointing to sensitivity with respect to the preparation. For instance, the experimental scatter could be caused by different degrees of disorder in the samples, as observed for Co<sub>2</sub>FeAl earlier.<sup>26</sup> Also, the calculated data confirm such a sensitivity; while the total moment of Mn-containing compounds is almost insensitive to lattice expansion, the Fe-containing compounds show considerably different moments at  $a^{\text{LSDA}}$  and  $a^{\text{expt.}}$ , respectively. To be specific, LSDA+OP(b) data will be compared with experiment, since this approach describes the  $M_I/M_s$  ratio reasonably well.

The calculated total moments of Co<sub>2</sub>FeAl, Co<sub>2</sub>FeGa, and Co<sub>2</sub>FeGe are close to (at  $a^{\text{LSDA}}$ ) or moderately larger than (at  $a^{\text{expt.}}$ ) the measured ones. On the other hand, the calculated total moments of Co<sub>2</sub>FeSi are within the scatter of the experimental moments. Most obvious is the large dependence of the total moment of Co<sub>2</sub>FeSi on the lattice spacing: it

changes by 10% between theoretical and experimental lattice constant.

The reason for this sensitivity is elucidated in Fig. 3. At the theoretical lattice constant, the Fermi level is situated in a steep slope at the band edge of an almost empty minority spin  $3d$  band. The related band structure is shown in Fig. 4 and compared with the band structure of Co<sub>2</sub>MnSi. The dominating spin character of the states is indicated by red dashed lines (majority) and blue full lines (minority). Spin-orbit interaction mixes the spins, but this effect is small in the considered  $3d$  elements, see Sec. III E. At the Fermi

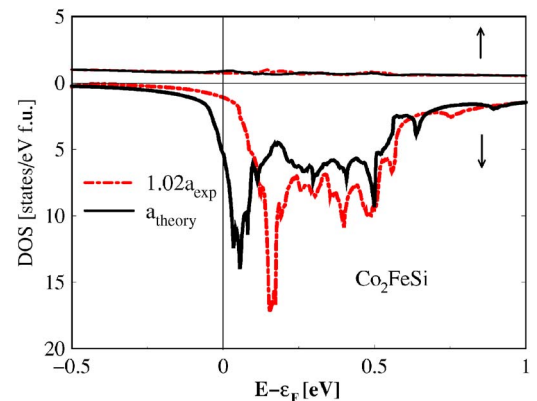


FIG. 3. (Color online) Density of states of Co<sub>2</sub>FeSi close to the Fermi level, evaluated for two different lattice parameters. Theoretical lattice parameter: full black lines; 1.02-fold experimental lattice parameter: dashed red lines. Majority (minority) spin DOS are given in the upper (lower) part of the figure.

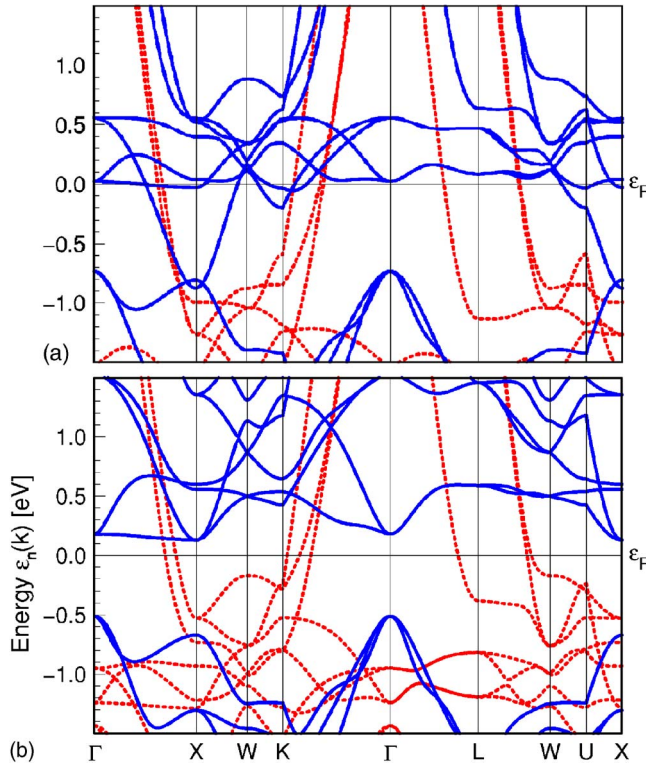


FIG. 4. (Color online) Band structure of  $\text{Co}_2\text{FeSi}$  (upper panel) and  $\text{Co}_2\text{MnSi}$  (lower panel) close to the Fermi level. The spin character is indicated by the red dashed lines (majority spin) and blue full lines (minority spin).

level, almost pure majority spin bands are present in  $\text{Co}_2\text{MnSi}$ , whereas flat minority spin bands cross the Fermi level in  $\text{Co}_2\text{FeSi}$ . The latter give rise to the discussed steep band edge (Fig. 3) and thus to the sensitivity of the magnetic moment of  $\text{Co}_2\text{FeSi}$  with respect to the lattice spacing. Similar flat bands are present in  $\text{Co}_2\text{MnSi}$  as well, but here they are unoccupied due to the larger exchange splitting of Mn in comparison with Fe.

If the volume of  $\text{Co}_2\text{FeSi}$  is increased, the flat minority spin band becomes more narrow and is further emptied. In turn, the exchange splitting increases, reinforcing the magnetovolume effect. At a lattice constant slightly larger than the experimental one, the band is empty (Fig. 3, red dashed line). The resulting dependence of the total moment on the lattice parameter in all three employed approximations is shown in Fig. 5. An expansion of slightly more than 1% beyond the experimental lattice parameter brings the calculated LSDA+OP(b) moment into the range defined by the experimental error bounds of the newest data.<sup>28</sup> At this spacing, the ratios  $M_I/M_S$ , calculated with LSDA+OP(b), amount to 0.08 for Co and 0.045 for Fe, in very nice agreement with the experimental values of 0.1 and 0.05, respectively.<sup>28</sup> This model dependence of the magnetic moment on the lattice parameters could be experimentally checked under pressure to decide whether  $\text{Co}_2\text{FeSi}$  is a half metal or not.

These results suggest an alternative explanation of the measured integer total moment of  $\text{Co}_2\text{FeSi}$ , contrasting the suggested correlation-induced half metallicity. While the LDA+ $U$  approach yields a half metallic state with an integer

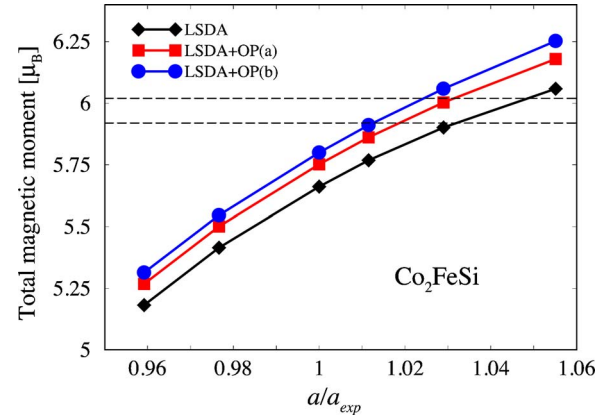


FIG. 5. (Color online) Volume dependence of the calculated total magnetic moment of  $\text{Co}_2\text{FeSi}$ . LSDA: black line with diamonds; LSDA+OP(a): red line with squares; LSDA+OP(b): blue line with bullets. The dashed lines show the range of experimental errors in Ref. 28 [ $(5.97 \pm 0.05)\mu_B$  at  $T=5$  K].

total moment and a total orbital moment of about  $0.2\mu_B$  at the experimental lattice constant,<sup>28</sup> the LSDA+OP(b) approach yields the experimental total moment at a 1.5–2% expanded lattice constant, and a total orbital moment of about  $0.35\mu_B$ . This is close to the experimental value of about  $0.45\mu_B$ , estimated from the measured moment ratios and the calculated site spin moments given in Ref. 28. The degree of spin polarization at the Fermi level (see Sec. III E) is very small in the suggested alternative approach, see Fig. 3.

What remains open is the question of why a lattice expansion is needed to simulate the experimental situation. It is clear from Fig. 3, that the electronic structure of well-ordered  $\text{Co}_2\text{FeSi}$  at theoretical lattice spacing bears a tendency toward enhancement of the magnetic moment. A small site disorder, that cannot be completely excluded on the basis of the existing data,<sup>28</sup> could provide such a moment enhancement, as it was found for the sister compound  $\text{Co}_2\text{FeAl}$ ,<sup>26</sup> which is much less susceptible to parameter changes than  $\text{Co}_2\text{FeSi}$ , see Table III.

Summarizing this section, we propose that the measured moment of  $\text{Co}_2\text{FeSi}$  need not be caused by a correlated half metallic state. It could, e.g., arise from a small but influential disorder of the sample. In the latter case, the spin polarization at Fermi level would be very small.

### E. Half metallicity

We have finally studied the effect of spin-orbit coupling and orbital polarization on the half metallicity of the considered full Heusler alloys. The spin-polarization degree (SPD) of the density of states (DOS) is defined by

$$\text{SPD} = \frac{n^\uparrow(\epsilon_F) - n^\downarrow(\epsilon_F)}{n^\uparrow(\epsilon_F) + n^\downarrow(\epsilon_F)}, \quad (6)$$

where  $n^\sigma(\epsilon_F)$  corresponds to majority ( $\uparrow$ ) and minority ( $\downarrow$ ) spin DOS at the Fermi level. In Table IV, we present the SPD values in percent, with and without spin-orbit coupling

TABLE IV. Spin-polarization degree for half ferromagnetic  $\text{Co}_2\text{YZ}$  full Heusler alloys. SPD values at LSDA lattice constants without spin-orbit coupling (SO: no) and with spin-orbit coupling (SO: yes) are given in percent.

Y	SO	Al	Si	Ga	Ge
Mn	no	97	100	81	100
	yes	95	97	81	99
Fe	no	39	-77	43	-67
	yes	38	-72	41	-65

at LSDA lattice constants. Recall, in perfect half metals, SPD amounts to 100%. According to our band-structure calculations, only  $\text{Co}_2\text{MnSi}$  and  $\text{Co}_2\text{MnGe}$  are fully spin polarized in the absence of spin-orbit coupling. However, spin-orbit coupling reduces SPD by 3% and 1%, respectively, for those intermetallic compounds. Adding OP corrections to the LSDA-XC functional does not significantly change the spin-polarization degree.

Moreover, the calculated SPD values for the considered compounds indicate that the Mn-based full Heusler alloys seem to be more suitable candidates for half metallicity, whereas SPD values for Fe-based full Heusler alloys considerably deviate from 100%. For instance,  $\text{Co}_2\text{FeSi}$  has a relatively large negative SPD value at LSDA lattice constant. From Fig. 3 and the discussion in previous section it is, however, obvious that lattice expansion considerably reduces the SPD value.

Recently, Karthik *et al.*<sup>51</sup> have shown in their point-contact Andreev reflection (PCAR) experiments that  $\text{Co}_2\text{FeAl}$  is a normal ferromagnet with PCAR spin polarization value of 56%. This finding is in qualitative agreement with our result (SPD 38%) and KKR result (30%) obtained by Miura *et al.*<sup>5</sup> One should note that there is no one-to-one correspondence between PCAR data and SPD values obtained from the DOS.<sup>52</sup> Only in an ideal half metal are both values equal to 100%. Note further that the measurement of spin-polarization value at the Fermi level is a quantity very sensitive to the sample preparation. Picozzi *et al.* have shown that defects such as Mn and Co antisites destroy the half metallicity for  $\text{Co}_2\text{MnSi}$  and  $\text{Co}_2\text{MnGe}$ .<sup>53</sup>

Concerning  $\text{Co}_2\text{FeGa}$ , our calculated SPD (41%) falls in between two other calculated values (37%, LMTO-ASA cal-

culated by Umetsu *et al.*;<sup>54</sup> 58%, FLAPW result by Zhang *et al.*<sup>21</sup>). All these results qualitatively match the related PCAR data (58%).<sup>21</sup>

The fully ordered  $\text{Co}_2\text{MnSi}$  with  $L2_1$  structure is predicted to be a half metal in our calculations which is in good agreement with LSDA results obtained by Ishida *et al.*<sup>16</sup> with the LMTO-ASA method and by Kandpal *et al.*<sup>29</sup> with the FLAPW approach. In contrast with these theoretical predictions, Ritchie *et al.* in their PCAR experiments have found that  $\text{Co}_2\text{MnSi}$  is a normal ferromagnet with PCAR spin polarization of 55%.<sup>20</sup> As they discussed the PCAR values are strongly dependent on surface segregation and disorder.

#### IV. SUMMARY AND CONCLUSIONS

Density functional FPLO calculations were performed for  $\text{Co}_2\text{YZ}$  ( $Y=\text{Mn, Fe}$ , and  $Z=\text{Al, Si, Ga, Ge}$ ) full Heusler alloys. We have calculated the spin and orbital moments of individual components in each compound including spin-orbit coupling and two variants of orbital polarization corrections.

Calculated orbital moments are in a reasonable agreement with experiment if orbital polarization corrections are taken into account. A rigid-band model for the orbital moment yields the wrong sign in the case of half metals. Considering changes of the character of ligand field states split by spin-orbit interaction yields orbital moments with the correct sign and order of magnitude, but a single ligand field parameter does not provide quantitative agreement with the full calculations. A large value of about  $0.18\mu_B$  is predicted for the Fe orbital moment in  $\text{Co}_2\text{FeGe}$ . Further experiments to check this prediction are desirable. An explanation is proposed for the recently measured total moment of  $\text{Co}_2\text{FeSi}$  and its orbital contributions. This explanation relies on a combination of orbital polarization enhancement (mainly driven by exchange) and residual site disorder. It predicts almost balanced spin-up and spin-down densities of states.

#### ACKNOWLEDGMENTS

We thank Warren E. Pickett, Gerhard Fecher, Sabine Wurmehl, and Yury Dedkov for very useful discussions. Financial support by Deutsche Forschungsgemeinschaft Schwerpunktprogramm 1145, is gratefully acknowledged.

<sup>1</sup>M. S. Lund, J. W. Dong, J. Lu, X. Y. Dong, C. J. Palmström, and C. Leighton, *Appl. Phys. Lett.* **80**, 4798 (2002).

<sup>2</sup>H. J. Elmers, G. H. Fecher, D. Valdaitsev, S. A. Nepijko, A. Gloskovskii, G. Jakob, G. Schönhense, S. Wurmehl, T. Block, C. Felser, P. C. Hsu, W. L. Tsai, and S. Cramm, *Phys. Rev. B* **67**, 104412 (2003).

<sup>3</sup>C. Felser, B. Heitkamp, F. Kronast, D. Schmitz, S. Cramm, H. A. Dürr, H. J. Elmers, G. H. Fecher, S. Wurmehl, T. Block, D. Valdaitsev, S. A. Nepijko, A. Gloskovskii, G. Jakob, G. Schönhense, and W. Eberhardt, *J. Phys.: Condens. Matter* **15**, 7019 (2003).

<sup>4</sup>X. Y. Dong, C. Adelman, J. O. Xie, C. J. Palmström, X. Lou, J. Strand, P. A. Crowell, J. P. Barnes, and A. K. Petford-Long, *Appl. Phys. Lett.* **86**, 102107 (2005).

<sup>5</sup>Y. Miura, K. Nagao, and M. Shirai, *Phys. Rev. B* **69**, 144413 (2004).

<sup>6</sup>S. J. Hashemifar, P. Kratzer, and M. Scheffler, *Phys. Rev. Lett.* **94**, 096402 (2005).

<sup>7</sup>A. T. Zayak and P. Entel, *J. Magn. Magn. Mater.* **290-291**, 874 (2005).

<sup>8</sup>Y. Kurtulus, R. Dronskowski, G. D. Samolyuk, and V. P. Antropov, *Phys. Rev. B* **71**, 014425 (2005).



- <sup>9</sup>F. Heusler, Verh. Dtsch. Phys. Ges. **5**, 219 (1903).
- <sup>10</sup>J. Kübler, A. R. Williams, and C. B. Sommers, Phys. Rev. B **28**, 1745 (1983).
- <sup>11</sup>R. A. de Groot, F. M. Mueller, P. G. van Engen, and K. H. J. Buschow, Phys. Rev. Lett. **50**, 2024 (1983).
- <sup>12</sup>J. M. D. Coey, M. Venkatesan, and M. A. Bari, in *Lecture Notes in Physics*, edited by C. Berthier, L. P. Levy, G. Martinez (Springer-Verlag, Heidelberg, 2002), Vol. 595, pp. 377–396.
- <sup>13</sup>C. M. Fang, G. A. de Wijs, and R. A. de Groot, J. Appl. Phys. **91**, 8340 (2002).
- <sup>14</sup>J. Grabis, A. Bergmann, A. Nefedov, K. Westerholt, and H. Zabel, Phys. Rev. B **72**, 024437 (2005).
- <sup>15</sup>H. Eschrig and W. E. Pickett, Solid State Commun. **118**, 123 (2001).
- <sup>16</sup>S. Ishida, S. Fujii, S. Kashiwagi, and S. Asano, J. Phys. Soc. Jpn. **64**, 2152 (1995).
- <sup>17</sup>S. Picozzi, A. Continenza, and A. J. Freeman, Phys. Rev. B **66**, 094421 (2002).
- <sup>18</sup>I. Galanakis, J. Phys.: Condens. Matter **16**, 3089 (2004).
- <sup>19</sup>I. Galanakis, P. H. Dederichs, and N. Papanikolaou, Phys. Rev. B **66**, 174429 (2002).
- <sup>20</sup>L. Ritchie, G. Xiao, Y. Ji, T. Y. Chen, C. L. Chien, M. Zhang, J. Chen, Z. Liu, G. Wu, and X. X. Zhang, Phys. Rev. B **68**, 104430 (2003).
- <sup>21</sup>M. Zhang, E. Brück, F. R. de Boer, Z. Li, and G. Wu, J. Phys. D **37**, 2049 (2004).
- <sup>22</sup>Ph. Mavropoulos, K. Sato, R. Zeller, P. H. Dederichs, V. Popescu, and H. Ebert, Phys. Rev. B **69**, 054424 (2004).
- <sup>23</sup>Ph. Mavropoulos, I. Galanakis, V. Popescu, and P. H. Dederichs, J. Phys.: Condens. Matter **16**, S5759 (2004).
- <sup>24</sup>H. J. Elmers, S. Wurmehl, G. H. Fecher, G. Jakob, C. Felser, and G. Schönhense, J. Magn. Magn. Mater. **272**, 758 (2004).
- <sup>25</sup>H. J. Elmers, S. Wurmehl, G. H. Fecher, G. Jakob, C. Felser, and G. Schönhense, Appl. Phys. A: Mater. Sci. Process. **79**, 557 (2004).
- <sup>26</sup>S. Wurmehl, G. H. Fecher, K. Kroth, F. Kronast, H. A. Dürr, Y. Takeda, Y. Saitoh, K. Kobayashi, H. Lin, G. Schönhense, and C. Felser, J. Phys. D **39**, 803 (2006).
- <sup>27</sup>K. Miyamoto, A. Kimura, K. Iori, K. Sakamoto, T. Xie, T. Moko, S. Qiao, M. Taniguchi, and K. Tsuchiya, J. Phys.: Condens. Matter **16**, S5797 (2004).
- <sup>28</sup>S. Wurmehl, G. H. Fecher, H. C. Kandpal, V. Ksenofontov, C. Felser, H. J. Lin, and J. Morais, Phys. Rev. B **72**, 184434 (2005).
- <sup>29</sup>H. C. Kandpal, G. H. Fecher, C. Felser, and G. Schönhense, Phys. Rev. B **73**, 094422 (2006).
- <sup>30</sup>I. Galanakis, Phys. Rev. B **71**, 012413 (2005).
- <sup>31</sup>P. Hohenberg and W. Kohn, Phys. Rev. **136**, B864 (1964).
- <sup>32</sup>I. Opahle, Ph.D. thesis, Technische Universität Dresden, 2001. H. Eschrig, M. Richter, and I. Opahle, in *Relativistic Electronic Structure Theory-Part II: Applications*, edited by P. Schwerdtfeger (Elsevier, Amsterdam, 2004), pp. 723–776.
- <sup>33</sup>FPLO-5.10-20 [improved version of the original FPLO code by K. Koepnick and H. Eschrig, Phys. Rev. B **59**, 1743 (1999)]; <http://www.FPLO.de>.
- <sup>34</sup>J. P. Perdew and Y. Wang, Phys. Rev. B **45**, 13244 (1992).
- <sup>35</sup>M. Richter, in *Handbook of Magnetic Materials*, edited by K. H. J. Buschow (Elsevier, Amsterdam, 2001), Vol. 13.
- <sup>36</sup>H. Eschrig, M. Sargolzaei, K. Koepnick, and M. Richter, Europhys. Lett. **72**, 611 (2005).
- <sup>37</sup>O. Eriksson, M. S. S. Brooks, and B. Johansson, Phys. Rev. B **41**, 7311 (1990).
- <sup>38</sup>P. Villars and L. D. Calvert, *Pearson's Handbook of Crystallographic Data for Intermetallic Phases*, 2nd Edition (ASM International, Ohio 1991).
- <sup>39</sup>J. Kübler, *Theory of Itinerant Electron Magnetism* (Oxford Science Publications, Oxford, 2000).
- <sup>40</sup>C. T. Chen, Y. U. Idzerda, H. J. Lin, N. V. Smith, G. Meigs, E. Chaban, G. H. Ho, E. Pellegrin, and F. Sette, Phys. Rev. Lett. **75**, 152 (1995).
- <sup>41</sup>B. T. Thole, P. Carra, F. Sette, and G. van der Laan, Phys. Rev. Lett. **68**, 1943 (1992).
- <sup>42</sup>P. Carra, B. T. Thole, M. Altarelli, and X. Wang, Phys. Rev. Lett. **70**, 694 (1993).
- <sup>43</sup>A. Scherz, H. Wende, K. Baberschke, J. Minár, D. Benea, and H. Ebert, Phys. Rev. B **66**, 184401 (2002).
- <sup>44</sup>I. Tchapyguine, Ph.D. thesis, Technische Universität Dresden, 2002.
- <sup>45</sup>O. Eriksson, L. Nordström, A. Pohl, L. Severin, A. M. Boring, and B. Johansson, Phys. Rev. B **41**, 11807 (1990).
- <sup>46</sup>H. Ebert, R. Zeller, B. Drittler, and P. H. Dederichs, J. Appl. Phys. **67**, 4576 (1990).
- <sup>47</sup>K. H. J. Buschow, P. G. van Engen, and R. Jongebreur, J. Magn. Magn. Mater. **38**, 1 (1983).
- <sup>48</sup>V. Niculescu, J. I. Budnick, W. A. Hines, K. Raj, S. Pickart, and S. Skalski, Phys. Rev. B **19**, 452 (1979).
- <sup>49</sup>P. J. Webster, J. Phys. Chem. Solids **32**, 1221 (1971).
- <sup>50</sup>T. Ambrose, J. J. Krebs, and G. A. Prinz, J. Appl. Phys. **87**, 5463 (2000).
- <sup>51</sup>S. V. Karthik, A. Rajanikanth, Y. K. Takahashi, T. Okhubo, and K. Hono, Appl. Phys. Lett. **89**, 052505 (2006).
- <sup>52</sup>I. I. Mazin, Phys. Rev. Lett. **83**, 1427 (1999).
- <sup>53</sup>S. Picozzi, A. Continenza, and A. J. Freeman, Phys. Rev. B **69**, 094423 (2004).
- <sup>54</sup>R. Y. Umetsu, K. Kobayashi, A. Fujita, K. Oikawa, R. Kainuma, K. Ishida, N. Endo, K. Fukamichi, and A. Sakuma, Phys. Rev. B **72**, 214412 (2005).